AN ANALYSIS OF BOGIE HUNTING INSTABILITY

Traian MAZILU[1]

Mişcarea de şerpuire este specifică vehiculelor feroviare şi instabilitatea ei limitează viteza maximă de circulaţie. Articolul se ocupă de mişcarea de şerpuire a unui boghiu care echipează vagoanele de călători. Pentru aceasta, s-a considerat un model complex pentru boghiu şi cale. Mişcarea de şerpuire este cuplată cu mişcarea verticală. Datorită contactului roată-şină, mişcarea de şerpuire este neliniară. Pentru studierea ciclurilor limită este aplicată teoria bi-contactului elastic roată-şină. Mişcarea de şerpuire a boghiului are două cicluri limită. Primul ciclu limită este instabil, fără ca flancul exterior al profilului roţii să atingă flancul interior al şinei. Al doilea ciclu limită este stabil pentru că şinele limitează deplasarea transversală a osiilor. Este studiată de asemenea mişcarea de şerpuire a boghiului pe o cale cu abateri de aliniament aleatoare.

The hunting movement is specific for railway vehicles and their maximal speed is limited due to hunting instability. The paper deals with the hunting movement of passenger coach bogie. To this aim, a complex bogie/track model has been considered. The hunting and the vertical movements are coupled. The hunting movement is non-linear due to wheel/rail contact. To study the hunting limit cycles, the elastic wheel/rail bi-contact theory is applied. The bogie hunting exhibits two limit cycles. The first is unstable and no contact wheel flange/rail occurs. The second limit cycle is stable due to wheel flange/rail impact. The hunting movement on a track which has random alignment irregularities is studied as well.

Keywords: bogie, hunting, stability, limit cycle, random defects

1. Introduction

The hunting movement is a consequence of the reversed conic shape of the rolling surfaces. For instance, if the axle is transversally displaced, the wheel rolling on a larger diameter will advance quicker than the other one, which always stays behind because the wheels are fixed in a rigid manner to the axle's body (fig.1). The axle spins compared to the vertical axis and, eventually, will approach the track's middle axis. In this moment, the axle spinning angle will be at its highest value and both wheels will roll on even diameters. Next, the axle will continue its movement, leaving the center position to the opposite side from the initial lateral displacement, forcing the wheel to roll on smaller and smaller

[1] Reader, Dept. of Railway Vehicles, University POLITEHNICA of Bucharest, Romania, e-mail: trmazilu@yahoo.com

diameters and the other one on increasingly larger diameters. Both wheels will reach the same level at the precise moment when the axle center is situated at the maximum distance from the rail longitudinal axis. From now on, the movement will repeat itself in reverse. The axle center's trajectory is a sinuous curve.

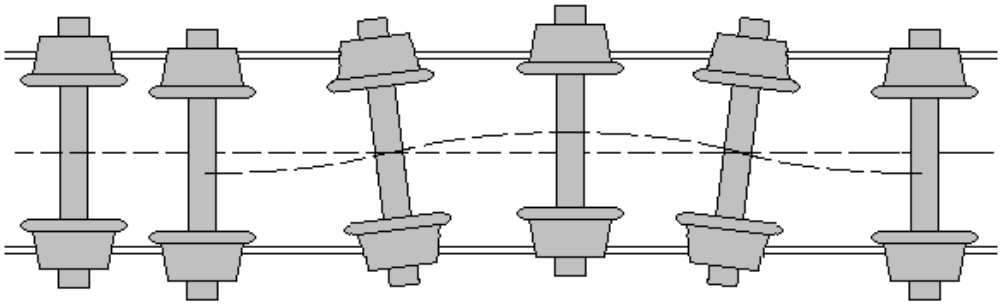

1. The axle trajectory.

This phenomenon of kinematical motion was described for the first time by Stephenson, and Klingel [1] determined the hunting wavelength according to his famous formulae

$$L = 2\pi\sqrt{\frac{re}{\gamma_e}}, \tag{1}$$

where r is the rolling radius, $2e$ – the distance between the wheel/rail contact points and γ_e – the effective conicity.

This movement is passed over to the bogie and to the vehicle body through suspension elements. During the circulation, this hunting movement is also sustained by rail alignment irregularities; therefore, its intensity will be influenced by the size of these irregularities. In addition to that, the regime of this hunting movement depends on the running speed - at low speeds, this movement is stable and at high speeds, this movement becomes unstable. The value of speed when the movement behaviour becomes unstable is known as the so-called *hunting critical speed*. Above the critical speed, large values of forces acting between wheel and rail occur, and the resultant of these forces contribute to: the risk of derailment at higher speeds, damage to track, high level of vibration, with bad ride comfort or damage to freight, fatigue failure of the vehicle structure and wear of components.

The hunting stability and critical speed were studied and linear models have been used in many papers. Wickens [2, 3], Joly [4, 5], Sebeşan [6] or Lee

and Cheng [7] investigated the influence of different parameters to create a basis for better bogie design.

The hunting movement is an interesting example of non-linear vibration. The non linearity of the movement is governed by the laws of geometry and friction. Generally, the wheel/rail contact is represented by a point on the rolling surface (the so-called *mono – contact*), as it may be seen in fig. 2. If the axle consumes its lateral displacement, the flange of the attacking wheel will touch the interior flange of the rail. This particular situation is known as *bi – contact* and occurs when there are two actual contact points between the wheel and the rail. When the movement stability is lost, the oscillation is limited in amplitude by the wheel flanges and a limit cycle occurs.

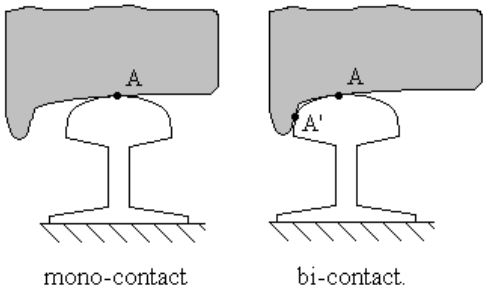

Fig. 2. The wheel/rail contact.

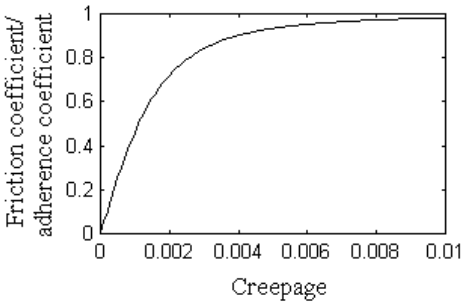

Fig. 3. Wheel/rail friction coefficient.

On the other hand, the friction force has a non – linear variation, which depends on the so-called *creepage* (the ratio between the wheel slip speed and the wheel rolling velocity) when the wheel approaches to the appropriate rail as one can see in fig. 3.

Non – linear models were used by De Pater [8] and van Bommel [9]. They applied harmonic balance method or method of Krylov and Bogoljubov to study the limit cycle due to flange/rail contact introduced as percussion. Huilgol [10], True and Kaas-Petersen, [11], and True, [12] investigated the Hopf bifurcation, taking into account the nonlinear wheel/rail contact force as well.

To predict the wheel/rail contact force during the hunting movement, Pascal [13] and Shabana et al. [14] developed their own methods. The critical point remains the wheel/rail bi-contact. An original approach of this issue has been introduced by Mazilu [15, 16]. Starting from this method, the limit cycles for bogie hunting are analyzed in this paper.

2. Mechanical model

The mechanical model of a two-axle bogie/track is presented in fig.4. The movement is considered to be reported to the fixed referential $\omega\xi\eta\zeta$. The bogie

moves along the ωξ axis at a constant velocity, V. The suspended mass of the bogie is considered to be a rigid with 5 degrees of freedom: two translations – *lateral displacement y* and *vertical displacement* (*bounce*) *z*; three rotations – *roll* φ, *gallop* θ and *yaw* ψ. The mass centre of the bogie is situated at axle level. Usually, modern passenger coaches fulfil this requirement.

The axles are rigid bodies with four degrees of freedom: two translations – *recoil* x_i and *lateral displacement* y_i – and two rotations – *the revolution* θ_i and *yaw* ψ_i with i=1÷2. The *vertical displacement* z_i and *roll* φ_i movements of the axle are not independent. The corresponding movement equations are though written, in order to be used in the calculus for reaction forces on the rolling surfaces. The gyroscopic effect of the axle is considered as well.

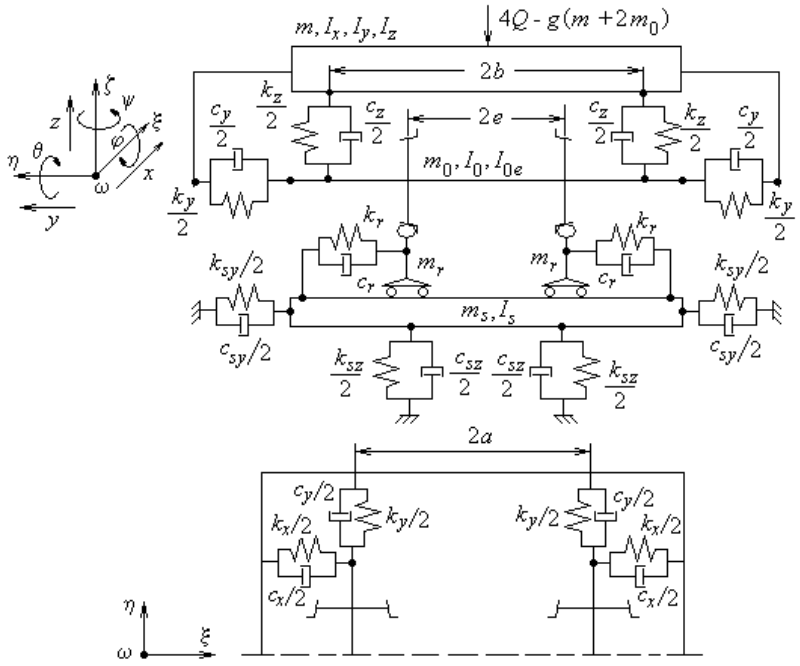

Fig. 4. The mechanical model for bogie hunting.

Under each axle, the track is considered as a rigid body system with three pieces, two rails and one sleeper, elastically connected together and to the ground. In parallel to the elastic elements, damping elements were considered as well. The periodic variation of the rail lateral stiffness caused by the periodic sleeper support is negligible. The rails have lateral independent movements y_{rij} (axle i, wheel j). The sleeper standing right under the 'i' axle moves transversally with y_{si}.

The sleeper and the rails are moving together in the vertical z_{si} movement and in the roll φ_{si} movement.

All elastic and damping elements have linear characteristics.

The equations of motion result through the application of the Lagrange equations method. The following were obtained:

1. The equations of motion of the bogie:

$$m\ddot{y} + c_y(2\dot{y} - \dot{y}_1 - \dot{y}_2) + k_y(2y - y_1 - y_2) = 0, \tag{1}$$

$$m\ddot{z} + c_z(2\dot{z} - \dot{z}_1 - \dot{z}_2) + k_z(2z - z_1 - z_2) = 0, \tag{2}$$

$$I_x\ddot{\varphi} + c_\varphi(2\dot{\varphi} - \dot{\varphi}_1 - \dot{\varphi}_2) + k_\varphi(2\varphi - \varphi_1 - \varphi_2) = 0, \tag{3}$$

$$I_y\ddot{\theta} + c_\theta\left(2\dot{\theta} + \frac{\dot{z}_1 - \dot{z}_2}{a}\right) + k_\theta\left(2\theta + \frac{z_1 - z_2}{a}\right) = 0, \tag{4}$$

$$\begin{aligned} &I_z\ddot{\psi} + c_{\psi x}(2\dot{\psi} - \dot{\psi}_1 - \dot{\psi}_2) + k_{\psi x}(2\psi - \psi_1 - \psi_2) + \\ &+ c_{\psi y}\left(2\dot{\psi} - \frac{\dot{y}_1 - \dot{y}_2}{a}\right) + k_{\psi y}\left(2\psi - \frac{y_1 - y_2}{a}\right) = 0, \end{aligned} \tag{5}$$

where m stands for the suspended bogie mass, I_x, I_y and I_z for the moments of inertia, k_x, k_y and k_z for the elastic constants, c_x, c_y and c_z for the damping constants, $2a$ for the bogie wheelbase, $2b$ for the transversal suspension base and $c_\varphi = c_z b^2$, $k_\varphi = k_z b^2$, $c_{\psi x} = c_x b^2$, $k_{\psi x} = k_x b^2$, $c_{\psi y} = c_y a^2$, $k_{\psi y} = k_y a^2$, $c_\theta = c_z a^2$ and $k_\theta = k_z a^2$;

2. The equations of motion of the axle 'i'

$$m_0\ddot{x}_i + c_x(\dot{x}_i - \dot{x}) + k_x(x_i - x) = X_{i1} + X_{i2}, \tag{6}$$

$$m_0\ddot{y}_i + c_y\left[\dot{y}_i - \dot{y} + (-1)^i a\dot{\psi}\right] + +k_y\left[y_i - y + (-1)^i a\psi\right] = Y_{i1} + Y_{i2}, \tag{7}$$

$$m_0\ddot{z}_i + c_z\left[\dot{z}_i - \dot{z} - (-1)^i a\dot{\theta}\right] + k_z\left[z_i - z - (-1)^i a\theta\right] = Q_{i1} + Q_{i2} - 2Q, \tag{8}$$

$$I_0\ddot{\theta} = -r(X_{i1} + X_{i2}), \tag{9}$$

$$I_{0e}\ddot{\varphi}_i + c_\varphi(\dot{\varphi}_i - \dot{\varphi}) + k_\varphi(\varphi_i - \varphi) - I_{0e}(V/r)\dot{\psi}_i = r(Y_{i1} + Y_{i2}) + e(Q_{i1} - Q_{i2}), \tag{10}$$

$$I_{0e}\ddot{\psi}_i + c_{\psi x}\left(\dot{\psi}_i - \dot{\psi}\right) + k_{\psi x}\left(\psi_i - \psi\right) + I_{0e}\left(V/r\right)\dot{\varphi}_i = -e\left(X_{i1} - X_{i2}\right), \tag{11}$$

where m_0 stands for the mass of the axle, I_0 and I_{0e} for the moments of inertia and X_{ij}, Y_{ij}, Q_{ij} for the projections of the resultant of the wheel/rail contact force;

3. The equations of motion of the track

- the equation of motion of the rail under wheel j of axle i

$$m_r\ddot{y}_{rij} + c_r(\dot{y}_{rij} - \dot{y}_{si}) + k_r(y_{rij} - y_{si}) = -Y_{ij} + (-1)^j Q\mathrm{tg}\gamma, \tag{12}$$

- the equations of motion of the sleeper under axle i

$$m_s\ddot{y}_{si} + c_{sy}\dot{y}_{si} + c_r\left(2\dot{y}_{si} - \dot{y}_{ri1} - \dot{y}_{ri2}\right) + k_{sy}y_{si} + k_r\left(2y_{si} - y_{ri1} - y_{ri2}\right) = 0, \tag{13}$$

$$\left(m_s + 2m_r\right)\ddot{z}_{si} + c_{sz}\dot{z}_{si} + k_{sz}z_{si} = 2Q - Q_{i1} - Q_{i2}, \tag{14}$$

$$\left(I_s + 2m_r e^2\right)\ddot{\varphi}_{si} + c_{sz}e_r^2\dot{\varphi}_{si} + k_{sz}e_r^2\varphi_{si} = -e\left(Q_{i1} - Q_{i2}\right), \tag{15}$$

where m_r stands for the mass of the rail, m_s for the mass of the sleeper, I_s for the moment inertia of the sleeper, k_r, k_{sy} and k_{sz} for the elastic constants, c_r, c_{sy}, and c_{sz} for the damping constants and $2Q$ for the static load of the axle.

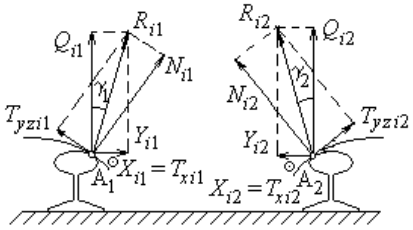

Fig. 5. The wheel/rail contact forces.

The wheel/rail contact forces are presented in fig.5 (mono – contact): the normal force N_{ij} and the friction force T_{ij} with its components T_{xij} and T_{yzij}. The components of the resultants of the contact forces are

$$X_{ij} = T_{xij} + \sigma\left(\delta_{fij}\right)T_{fij}, \tag{15}$$

$$\begin{aligned} Y_{ij} &= \mp N_{ij}\sin\left(\gamma_{ij} \pm \varphi_{si}\right) + T_{yzij}\cos\left(\gamma_{ij} \pm \varphi_{si}\right) + \\ &+ \sigma\left(\delta_{fij}\right)\left[\mp N_{fij}\sin\left(\gamma_f \pm \varphi_{si}\right) + T_{fyzij}\cos\left(\gamma_f \pm \varphi_{si}\right)\right], \end{aligned} \tag{16}$$

$$\begin{aligned} Q_{ij} &= N_{ij}\cos\left(\gamma_{ij} \pm \varphi_{si}\right) \pm T_{yzij}\sin\left(\gamma_{ij} \pm \varphi_{si}\right) + \\ &+ \sigma\left(\delta_{fij}\right)\left[N_{bij}\cos\left(\gamma_f \pm \varphi_{si}\right) \pm T_{fyzij}\sin\left(\gamma_f \pm \varphi_{si}\right)\right], \end{aligned} \tag{17}$$

where γ_{ij} stands for the contact angle, δ_{fij} for the elastic deformation of the wheel in case of flange contact (subscript *f*) and $\sigma(.)$ is the Heaviside function.

For the friction forces, the non – linear Chartet's modified formula [17] was used [6, 15, 18]

$$T_x = -\frac{\kappa\nu_x N}{\sqrt{1+(\kappa\nu/\mu)^2}},\ T_{yz} = -\frac{\kappa\nu_{yz} N}{\sqrt{1+(\kappa\nu/\mu)^2}}, \tag{18}$$

where ν_x and ν_{yz} stand for the components of the creepage known as ν, κ is the creepage coefficient determined in accordance to Kalker's theory [19] and μ is the coefficient of adherence. The creepage is determined mainly by the kinematics of the axle.

The system of equations may be solved numerically using the Runge – Kutta method. If both wheels of the same axle are in a mono – contact position, the normal forces are calculated from the algebraic system formed by the axle lifting and roll movement equations. These equations were obtained by substituting the accelerations of the dependent movements (z_i and φ_i) with the accelerations of the independent coordinates. The corresponding formulae result from kinematical analysis of the axle.

If one wheel is in a bi – contact position, the reaction force on the flange is an additional unknown value. The problem may be solved iterative, using the formula for the flange elastic deformations (Hertz). The elastic deformation of the flange is correlated with the axle and rail positions, which are known for each integration step. The elastic deformation of the flange is calculated according to the wheel/rail elastic bi – contact theory [15].

3. Numerical application

Next, the hunting movement of the Y32 bogie is analyzed. The bogie main parameters are: m = 3680 kg, I_x = 3680 kgm^2, I_y = 1200 kgm^2, I_z = 3800 kgm^2, k_x = 40 MN/m, k_y = 6 MN/m, k_z = 1.25 MN/m, c_x = 27 kN/(m/s), c_y = 10.5 kN/(m/s), c_z = 8.4 kN/(m/s), m_0= 1310 kg, I_0 = 740 kgm^2, I_{0e} = 210 kgm^2, $2e$ =1.5 m, $2a$ = 2.56 m, $2b$ = 2 m, r = 0.445 m, $2Q$ = 110 kN.

The track parameters are: m_r = 60 kg, m_s = 240 kg, I_s = 135 kgm^2, k_r =70 MN/m, k_{sy} = 70 MN/m, k_{sz} = 65 MN/m, c_r = 100 kN/(m/s), c_{sy} = 300 kN/(m/s), c_{sz}= 140 kN/(m/s). The CFR S 78 wheel profile and UIC 60 rail are considered.

Before solving the movement equations numerically, the critical hunting speed was calculated (linear model). The linear equation system has the following matrix structure:

$$\{\dot{\mathbf{q}}\} = \mathbf{A}\{\mathbf{q}\} \tag{19}$$

in which {**q**} is the column for state parameters and **A** is the system matrix. The eigenvalues of the matrix **A** were calculated compared to the speed. The real part of these values is negative at low speeds, which means that the bogie is stable. When this part becomes positive, the bogie becomes unstable and the (linear) critical speed may be determined. In this particular case, the critical speed is V_l = 69.6 m/s for an effective conicity of 0.124.

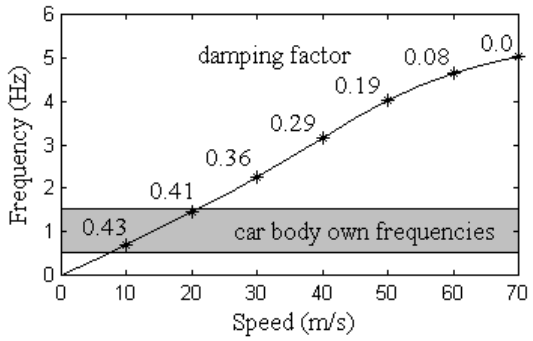

Fig. 6. Stability diagram.

Figure 6 presents the stability diagram for the bogie hunting. When the speed increases, the frequency increases as well. For the critical speed, a frequency of 5 Hz results. The previous value is much higher than the eigenfrequencies of car body (lateral displacement and yaw). This fact explains why the car body influence can be reduced to the dead load. The hunting wavelength has the range of 12.5-14.3 m. The values of the damping factor are presented as well. The damping decreases if the bogie speed increases, especially above the speed of 40 m/s.

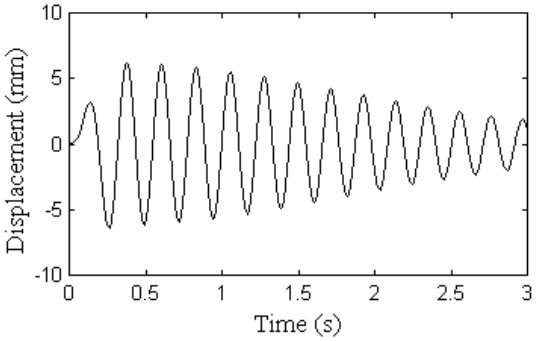

Fig. 7. The lateral displacement of the first axle
(u = 1.9 mm, λ= 18 m, V = 66.22 m/s).

In the case of numerical simulation (non – linear model), the bogie is supposed to pass over a local sinusoidal alignment defect with a length equal to the wavelength. Fig. 7 shows the lateral displacement of the first axle for

V = 66.22 m/s, defect amplitude: u = 1.9 mm and defect wavelength λ = 18 m. The movement is damped and the hunting of the bogie is stable.

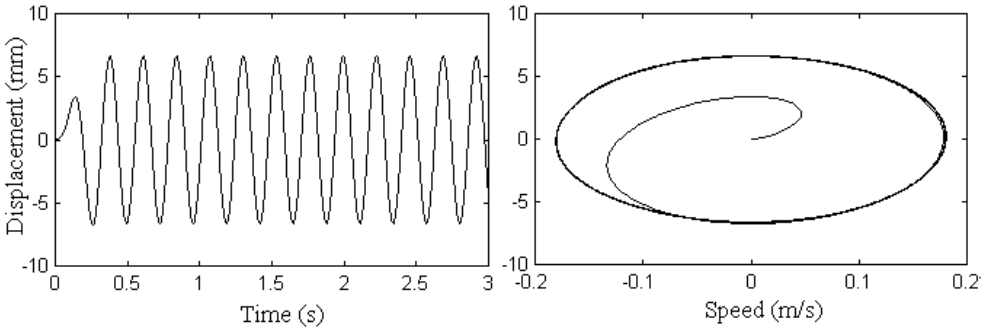

Fig. 8. The lateral displacement of the first axle (unstable limit cycle, $u = 2$ mm, $\lambda = 18$ m, $V = 66.22$ m/s).

Fig. 8 presents the lateral displacement of the first axle for V = 66.22 m/s, defect amplitude: 2 mm (more precisely, 1.9985 mm) and defect wavelength of 18 m. The movement has a constant amplitude of 6.63 mm and a frequency of 4.34 Hz. The trajectories in plane of the phase are closed curves - limit cycle. The axles do not touch the interior flange of the rail.

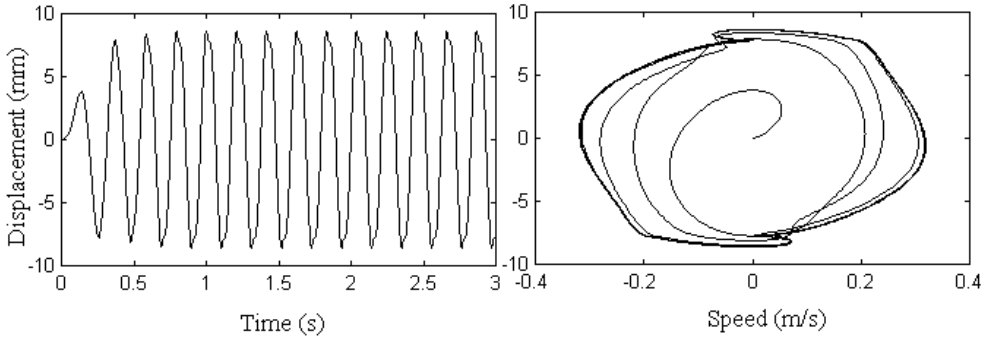

Fig. 9. The lateral displacement of the first axle (stable limit cycle $u = 2.1$ mm, $\lambda = 18$ m, $V = 66.2$ m/s).

If the defect amplitude increases to 2.1 mm, the movement amplitude increases along in time (see fig. 9). As a conclusion, the previous limit cycle (without touching the interior flange of the rail) is unstable.

On the other hand, the amplitude of the hunting movement increases until the wheels reach contact with the interior rail flange. The movement becomes again periodic and the phase trajectories are closed curves – another limit cycle was reached. The amplitude of this limit cycle is 8.2 mm for the first axle, and the frequency is 4.82 Hz.

When the wheel flange hits the rail, wheel/rail bi-contact occurs and the rolling surface is unloaded and the flange becomes loaded, increasing the risk of derailment. Fig. 10 displays this interesting aspect for the leading axle. Practically, the wheel/rail bi-contact occurs during a period of 27 ms. The normal force on wheel flange has a maximum value of 38.7 kN. Meanwhile, the normal force on the rolling surface decreases for short time from 64.3 kN to 41.0 kN.

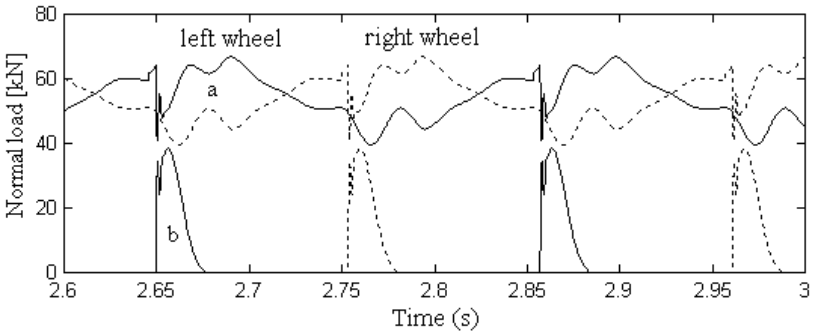

Fig. 10. The normal force: a) on the rolling surface; b) on the wheel flange.

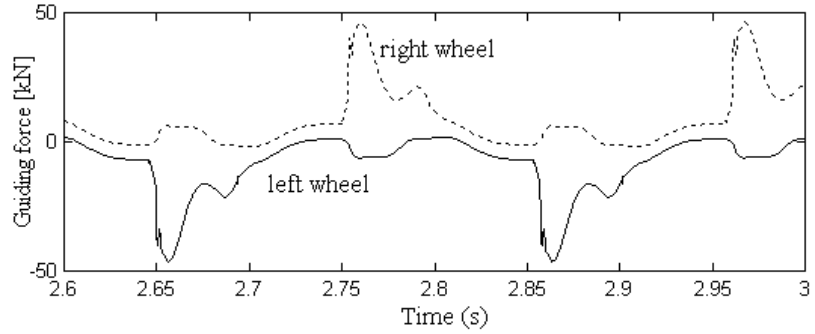

Fig. 11. The guiding forces on the first axle.

When the wheels reach contact with the interior rail flange, the guiding force (Y) increases as well. In dynamic of railway vehicles, the guiding force is of great importance. The ratio between the guiding force and the wheel load represents the derailment criterion. Further, the sum of guiding forces on the axle can contribute to the scraping of the track. Fig. 11 shows the time evolution of the guiding forces on the first axle. The maximum value is 46.3 kN, which means 84% of the dead load.

The whole rolling apparatus and the rails are also receiving tremendous shocks (fig. 12). The value lateral acceleration of the rail is very high under leading axle during stable limit cycle. The acceleration peak of 181 m/s^2 results from the numerical simulation.

The vibration behaviour of the two axles is intense as well. When the leading axle attacks a rail, the acceleration peak of 25 m/s^2 is calculated. For the trailing axle, the lateral acceleration level is lower, and as an instance, the peak has only 18 m/s^2.

Finally, the bogie vibration has a dangerous level for the vehicle structure. The lateral acceleration at the middle of the bogie has on effective value of 7.1 m/s^2. The same acceleration has its maximum value of 11.5 m/s^2.

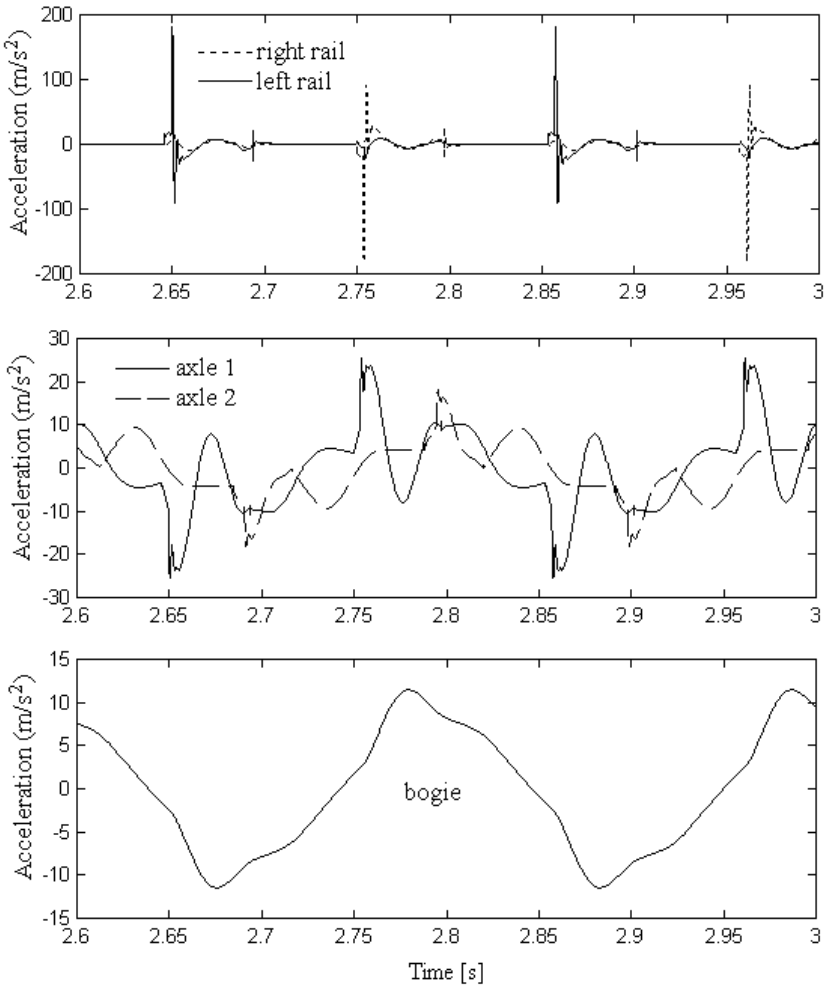

Fig. 12. Lateral accelerations.

If the amplitude of the defect is 4.6 mm, the wheel is completely unloaded and, as a consequence, the derailment occurs. For this reason, the limit cycle is *local stable*.

Figure 13 presents the Hopf diagram, the amplitude of limit cycle, either stable or unstable, versus the speed. The bogie hunting has two equilibrium solutions that depend on the value of the speed. For a bogie speed below V_{nl} = 61.5 m/s a solution without oscillation is the only existing equilibrium solution. For any initial excitation, the motion will be damped out. Certainly, this sentence remains true if no derailment occurs due to the extremely initial excitation. The speed V_{nl} is the *non-linear critical speed*.

In the speed range $V_{nl} < V < V_l$, there are two stable solutions and one unstable solution. The stable solutions are the equilibrium position and the limit cycle caused by the wheel/rail bi-contact. The unstable solution is the limit cycle without touching the interior rail flange. The existence of this unstable limit cycle shows that the hunting instability may occur even at speeds below the critical hunting speed V_l (linear model). The vehicle top speed must be small enough in order to avoid instability debut on accepted geometrical irregularities.

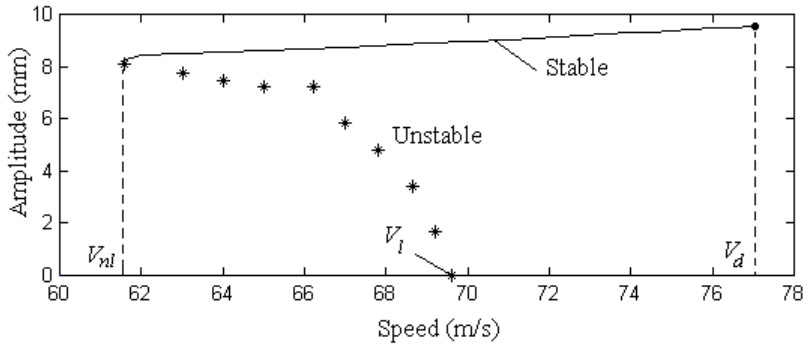

Fig. 13. Hopf bifurcation.

In the speed range $V_l < V < V_d$ = 77 m/s there is one stable solution, the limit cycle due to the bi-contact. For a bogie speed above V_d, the rolling surface is completely unloaded when the wheel smashes the rail and the derailment occurs.

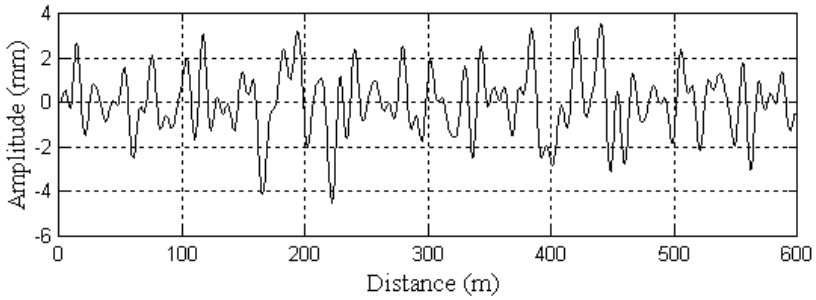

Fig. 14. The alignment defects.

The hunting on a track which has random alignment irregularities is studied. The studied sector has a length of 600 m and alignment defects of wavelengths from 10 to 82 m (fig. 14). The rail geometry is obtained through integration from the spectral density of the alignment defects. This spectral density has the following shape

$$S_u(\Omega) = \frac{A}{(B+\Omega)^3} \tag{20}$$

where Ω stands for the wave number, A and B are constants that minimize the error between the theoretical and the real (measured) spectre. The phases of the spectral components were randomly chosen between $-\pi$ and π. The efficient value for alignment defects is 1.38 mm. The track has local defects with amplitudes of about 4 mm. The quality level of this track is QN2 [20].

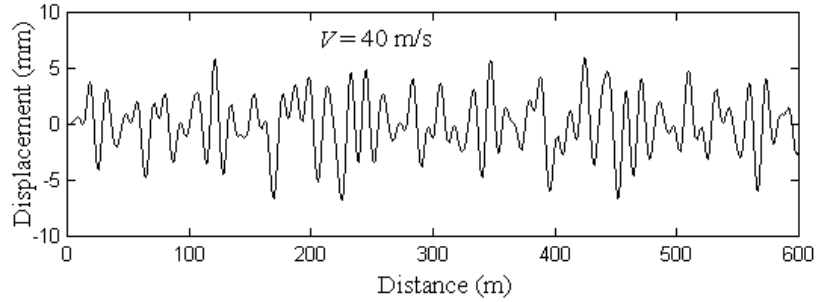

Fig. 15. The lateral displacement of the first axle,

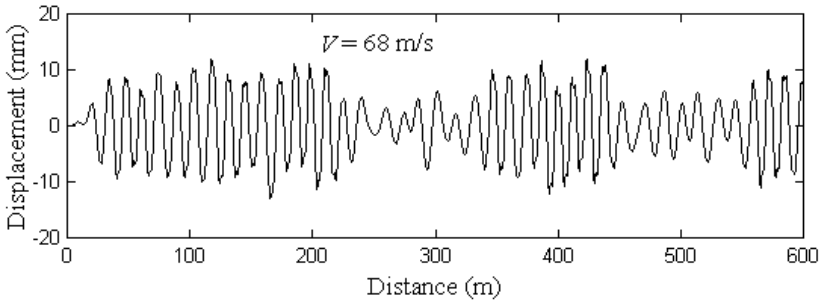

Fig. 16. The lateral displacement of the first axle,

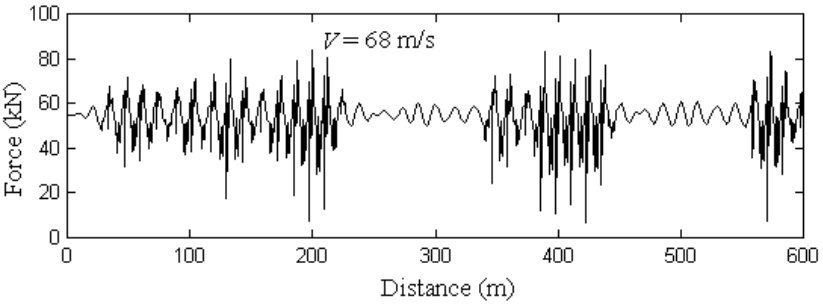

Fig. 17. The normal force on rolling surface of the first axle, the right wheel.

Figure 16 shows the lateral displacement of the first axle when running at $V = 40$ m/s. By comparing the two graphs shown in figures 14 and 15 it is easy to observe that the axle follows the alignment defects of the rail. The flange contact does not occur this time. The bogie's hunting is stable.

Figure 16 presents the displacement of the first axle when running at 67 m/s. The situation changes dramatically. After a very short time, the axle enters a limit cycles regime, at random amplitudes. The wheels are touching the interior rail flange and the normal force on the rolling surface decreases very much (fig. 17). For the bogie speed of 68 m/s, derailment occurs.

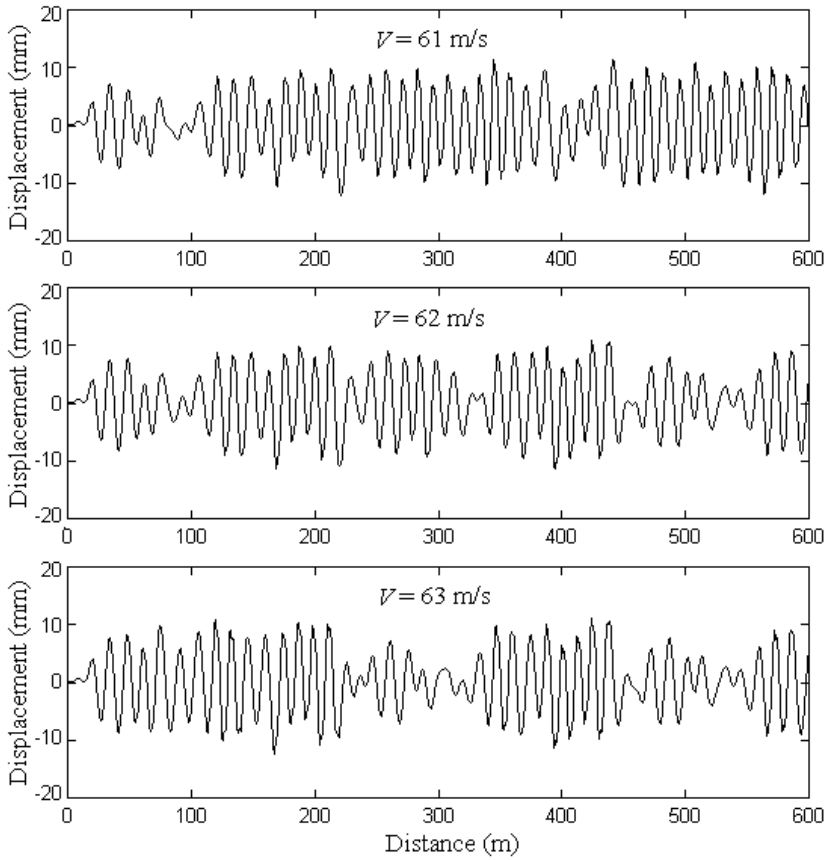

Fig. 18. Sensivity of simulated results to small changes in bogie speed. The lateral displacement of the first axle.

When the bogie speed is closed to the non-linear critical speed, the system is sensitive to speed due to the influence of unstable limit cycle. For instance, a minor change of the bogie speed significantly changes the running behaviour as

one can see in fig. 18. Pascal [21] met such phenomenon in his experimental works. This sensitivity makes difficult the validation of theoretical researches.

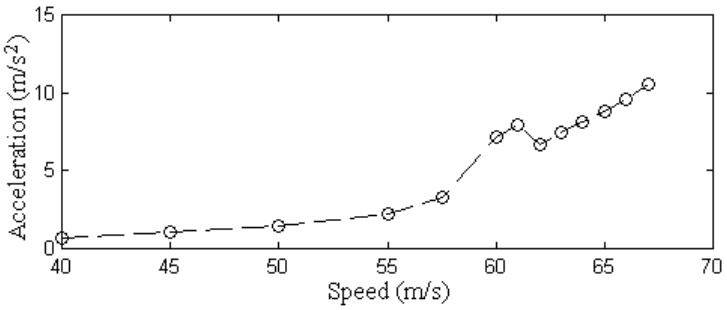

Fig. 19. The efficient acceleration of the axle.

The bogie's efficient acceleration increases weakly in the speed range lower than 55 m/s. But beyond this value, the efficient acceleration increases very much (fig. 18), and the bogie movement becomes unstable. When the bogie speed equals the non-linear critical speed, the acceleration has a local maximum due to the influence of unstable limit cycle. Practically, the unstable limit cycle meets the stable limit cycle and the effect is the higher dynamic behaviour.

4. Conclusions

The hunting movement of the railway vehicles is caused mainly by the conic wheel profiles and limits the top speed due to its instability. In this paper, the hunting of the Y 32 bogie was analyzed using an original method for calculation of the wheel/rail contact forces for both mono-contact and bi-contact cases.

The hunting has two limit cycles: an unstable mono-contact limit cycle and a locally stable bi-contact limit cycle. This last limit cycle is characterized by high accelerations and shocks.

The Hopf bifurcation diagram shows that the critical speed (linear) is located between the non-linear critical speed and the derailment speed.

The local alignment defects may lead to transitory unstable bogie hunting. Thus, the top speed has to be limited in order to avoid unstable vehicle hunting which starts to manifest before the non-linear critical speed.

The numerical simulation revealed the same hunting characteristics as in experimental tests.

R E F E R E N C E S

[1] *W. Klingel*, , Über den Lauf der Eisenbahnwagen auf gerader Bahn. Organ für die Fortschritte des Eisenbahnwesens, 20, 113-123, Table XXI, 1883.

[2] *A. H. Wickens*, The dynamic stability of railway vehicle wheelsets and bogies having profiled

wheels. Int. J. Solids Structures,1, 319-341, 1965.
[3] *A. H. Wickens*, The dynamics of railway vehicles on straight track: fundamental considerations of lateral stability. Proc. of the Institute of Mech. Engin., Vol. 180 (3F), 1-16, 1966.
[4] *R. Joly*, Étude de la stabilité transversale d'un véhicule ferroviaire circulant à grande vitesse. ORE DT 16/F Utrecht, octobre 1970.
[5] *R. Joly*, Turbotrain T.G.V. 001 Confort et stabilité transversale. Tome 1 Étude de la stabilité des bogies. Raport SNCF no 2, janvier 1973.
[6] *I. Sebeşan*, Dinamica vehiculelor de cale feerată, Bucureşti, Ed. Tehnică 1996, ediția a 2 a.
[7] *S.-Y. Lee*, *Y.-C. Cheng*, Hunting stability analysis of high-speed railway vehicle trucks on tangent tracks, Journal of Sound and Vibration 282, 881-898, 2005.
[8] *A. D. de Pater*, The approximate determination of the hunting movement of a railway vehicle by aid of the method of Krylov and Bogoliubov, Appl. Sci. Res. 10, 205-228, 1961. Paper delivered at the Xth International Congress of Appl. Mech. at Stresa, Aug, 31st to Sept. 7th, 1960.
[9] *P. van Bommel*, Application de la théorie des vibrations nonlineaires sur le problem du mouvement de lacet d'un vehicule de chemin de fer. Dissertation TH Delft, 1964.
[10] *R. R. Huilgol*, Hopf-Friedrichs bifurcation and the hunting of a railway axle, Quarterly Journal of Applied Mathematics 36, 85-94, 1978.
[11] *H. True*, *C. Kaas-Petersen*, A bifurcation analysis of nonlinear oscillations in railway vehicles, The Dynamics of Vehicles on Road and on Tracks, 8th IAVSD Symposium, 438-444, 1984.
[12] *H. True*, Some recent developments in nonlinear railway vehicle dynamics, 1st European Nonlinear Oscillation Conference, Proceedings of the International Conference, Hamburg, 129-148, 1993.
[13] *J. P. Pascal*, Calcul dynamic par VOCO des forces du contact roue/rail validation par les essais en lighe d'un wagon à essieux testé par la SNCF entre Hirson et Charleville. Rapport INRETS no 169, 1993.
[14] *A. Shabana*, *K. Zaazaa*, *J. Escalona*, *J. Sany*, Development of elastic force model for wheel/rail contact problems. Journal of Sound and Vibration 269, 295-325, 2004.
[15] *Tr.Mazilu*, Contribuții cu privire la studiul dinamic al interacțiunii dintre vehicul şi cale. Dizertație TH Bucureşti, 1999.
[16] *Tr.Mazilu*, Some aspects of the elastic wheel/rail bi-contact. Proc. of 9th IFToMM International Symposium on Theory of Machines and Mechanisms, Vol. II, 541-546, Bucharest, 2005.
[17] *A. Chartet*, Propriétés générales des contact de roulement. Théorie des similitudes. Compt. rend. Acad. Science, 225, 986-988, 1947.
[18] *G. Sauvage*, *C. Sartori*, Stabilité des vehicules à grande vitesse. Étude théorique de la dynamique transversale d'un bogie dans la voie. Revue Générale des Chemins de Fer apr. 207-225, 1977.
[19] *J. J. Kalker*, On the Rolling Contact of Two Elastic Bodies in the Presence of Dry Friction. Dissertation, TH Delft, 1967.
[20] Essais et homologation de vehicules ferroviaires du point de vue de comportement dynamique sécurité – fatigue de la voie – qualité de marche, Code UIC 518 OR, 2éme édition 01.10.1999.
[21] *J. P. Pascal*, Oscillations and chaotic behaviour of unstable railway wagons over large distances, Chaos, Solutions & Fractals 5 (9), 1725-1753, 1995.